Structural and functional alterations of muscle fibres in the novel mouse model of facioscapulohumeral muscular dystrophy

Giuseppe D'Antona[1], Lorenza Brocca[1], Orietta Pansarasa[1], Chiara Rinaldi[1], Rossella Tupler[2] and Roberto Bottinelli[1]

[1]*Department of Experimental Medicine and Interuniversity Institute of Myology (IIM), Human Physiology Unit, University of Pavia, Pavia, Italy*
[2]*Department of Biomedical Sciences, University of Modena and Reggio Emilia, Italy*

We recently generated a mouse model of facioscapulohumeral muscular dystrophy (FSHD) by selectively overexpressing *FRG1*, a candidate gene for FSHD, in skeletal muscle. The muscles of the FRG-1 mice did not show any plasmamembrane defect suggesting a novel pathogenetic mechanism for FSHD. Here, we study structure and function of muscle fibres from three lines of mice overexpressing *FRG1* at different levels: *FRG1*-low, *FRG1*-med, *FRG1*-high. Cross-sectional area (CSA), specific force (Po/CSA) and maximum shortening velocity (V_o) of identified types of muscle fibres from *FRG1*-low and *FRG1*-med mice were analysed and found to be lower than in WT mice. Fast fibres and especially type 2B fibres (the fastest type) were preferentially involved in the dystrophic process showing a much larger force deficit than type 1 (slow) fibres. Consistent with the latter observation, the MHC isoform distribution of several muscles of the three *FRG1* lines showed a shift towards slower MHC isoforms in comparison to WT muscle. Moreover, fast muscles showed a more evident histological deterioration, a larger atrophy and a higher percentage of centrally nucleated fibres than the soleus, the slowest muscle in mice. Interestingly, loss in CSA, Po/CSA and V_o of single muscle fibres and MHC isoform shift towards a slower phenotype can be considered early signs of muscular dystrophy (MD). They were, in fact, found also in *FRG1*-low mice which did not show any impairment of function *in vivo* and of muscle size *in vitro* and in soleus muscles, which had a completely preserved morphology. This study provides a detailed characterization of structure and function of muscle fibres in a novel murine model of one of the main human MDs and suggests that fundamental features of the dystrophic process, common to most MDs, such as the intrinsic loss of contractile strength of muscle fibres, the preferential involvement of fast fibres and the shift towards a slow muscle phenotype can occur independently from obvious alterations of the plasma membrane.

(Received 25 July 2007; accepted after revision 10 September 2007; first published online 13 September 2007)
Corresponding author G. D'Antona: Department of Experimental Medicine, Human Physiology Unit, University of Pavia, Via Forlanini 6, 27100 Pavia, Italy.   Email: gdantona@unipv.it

Muscular dystrophies (MDs) are a group of very heterogeneous genetic diseases characterized by skeletal muscle wasting and weakness. Most MDs have been linked to mutations in genes coding for proteins of the dystrophin-glycoprotein complex (DGC) (Durbeej & Campbell, 2002) or for enzymes likely to be involved in post-translational modification of such proteins (Muntoni *et al.* 2004). Whatever the mutation involved, the pathogenesis of most MDs can be traced back to a common path: a primary defect in the DGC would alter the link between cytoskeleton, plasmamembrane and extracellular matrix and would make muscle fibres more susceptible to contraction-induced damage. The latter phenomenon may depend either on a mechanical damage of the membrane and/or on altered ion homeostasis across the membrane ultimately bringing to calcium influx in muscle fibres and activation of proteolysis (Allen *et al.* 2005).

On the contrary, the genetic defect of facioscapulohumeral muscular dystrophy (FSHD), which is one of the three most common MDs, does not reside in any mutated genes. FSHD has been causally related to deletion of tandemly arrayed 3.3 kb repeat units (D4Z4) on chromosome 4q35. It has been shown that three genes located upstream of D4Z4, *FRG2*, *FRG1* and *ANT1*, which have not been found to be mutated in FSHD subjects, are overexpressed in FSHD-affected

human muscles (Gabellini *et al.* 2002). Very recently we demonstrated that transgenic overexpression of *FRG1* in skeletal muscle was sufficient to cause MD in mice, whereas mice overexpressing the two other candidate genes, *FRG2A*nd *ANT-1*, did not show clear signs of MD (Gabellini *et al.* 2006). Moreover, the link between MD manifestations and *FRG1* overexpression could not be ascribed to a plasma membrane defect, suggesting a novel pathogenetic mechanism for FSHD. However, similarly to other mouse models of MD, mice overexpressing *FRG1* (FSHD mice) showed impaired mobility *in vivo* and dystrophic features, which appeared differentially distributed among skeletal muscles.

In this respect, the analysis of the structure and function of muscle fibres from the FSHD mice is relevant for at least two reasons. It will further the understanding of a novel mouse model of one of the main human MDs which will be used in the future to further our knowledge on the pathogenesis of the disease and to develop therapeutic strategies. Furthermore, the FSHD mouse model may help understanding of whether and to what extent fundamental features of the dystrophic process at muscle fibre level, such as the intrinsic loss of contractile strength, the preferential involvement of fast fibres, and the fast to slow shift in muscle phenotype are necessarily linked to alterations of the DCG complex or can be a common path of alternative pathogenetic mechanisms. The FSHD mouse represents in fact one model of MD displaying histological and functional dystrophic features similar to the most studied models of MDs (Gabellini *et al.* 2006) which cannot be linked to a plasma membrane defect and ultimately to altered calcium homeostasis across the membrane (Allen *et al.* 2005). The absence of a clear plasmamembrane defect, as demonstrated by no change in serum creatine kinase (Richard *et al.* 2000) and lack in Evans blue uptake, is found in other murine models of MDs, as calpain-3 deficiency (Richard *et al.* 2000; Fougerousse *et al.* 2003). Nevertheless, murine models in which mutations do not involve proteins of the DCG complex either ultimately show membrane alterations such as the collagen VI deficient mouse (Bonaldo *et al.* 1998; Irwin *et al.* 2003) or do not show any clear sign of skeletal muscle involvement, such as the Six5 deficient mouse, a model of myotonic MD (Klesert *et al.* 2000; Sarkar *et al.* 2000). Notwithstanding the large body of information accumulating on murine models of MD, key features of the disease are still far from being fully understood.

In particular, muscle weakness is generally attributed to replacement of degenerating and necrotic muscle fibres with non contractile material (connective tissue and fat), which ultimately causes a loss of contractile muscle mass ('quantitative mechanism') even in the presence of increased muscle weight (pseudo-hypertrophy) (Watchko *et al.* 2002). Whether a 'qualitative mechanism', namely a loss of the intrinsic capacity to develop force by a given amount of muscle mass, is also involved in generating muscle weakness is unclear. In fact, whereas some earlier studies suggested no loss in specific force of single muscle fibres of *mdx* mice (Takagi *et al.* 1992; Lynch *et al.* 2000), more recently we consistently showed a clear Po/CSA deficit in several mouse models of MD: *mdx* (Denti *et al.* 2006), scid-*mdx* (Torrente *et al.* 2004), α-sarcoglycan null mice (Sampaolesi *et al.* 2003). Interestingly, in humans affected by Duchenne MD, whereas Fink *et al.* (1990) found an impairment of specific force of muscle fibres, Horowits *et al.* (1990) failed to show such impairment.

The origin of force loss in muscular dystrophies appears to be far from understood. In particular an imbalance between protein synthesis and breakdown towards increased proteolysis (McKeran *et al.* 1977; Elia *et al.* 1981; Warnes *et al.* 1981) and the replacement of necrotic cells by weaker regenerating fibres which show different functional characteristics from uninjured fibres may contribute to reduced capacity to generate force (Gregorevic *et al.* 2004). Furthermore, in intact fibres, decreased evoked calcium release due to ongoing triadic disruption might also contribute to force loss at least in *mdx* mice (Allen *et al.* 2005). In any case, in all muscular dystrophies the loss in force and specific force appear as common endpoints of diverse primary defects.

In addition, it is generally believed that the dystrophic processes preferentially strike fast fibres, and among fast fibres the fastest, type 2B fibres (Webster *et al.* 1988). However, such a preferential involvement has not been definitely demonstrated by the comparative analysis of strength of slow and fast muscle fibres.

As regards the origin of fibre deterioration in MDs, an increased calcium influx across membrane tears and calcium permeable leak channels followed by activation of proteolysis is a candidate mechanism (Allen *et al.* 2005; Yeung *et al.* 2005). Nevertheless it is still unclear what is the link between the genetic defect and muscle fibre deterioration, which are the cellular pathways involved and whether alternative mechanisms can be identified in the process (Gillis, 1999).

In this work, structure and function of identified types of single muscle fibres from the mouse model of FSHD were studied in comparison to corresponding types of WT fibres. The existence of several lines of FSHD, expressing *FRG1* at different levels and showing a variable progression of MD, enabled us to relate structural and functional properties of muscle fibres to the progression of the disease. Results of this study (i) provide a detailed characterization of skeletal muscle fibres of a novel mouse model of one of the main human MDs and (ii) point toward the existence of alternative pathogenetic mechanisms, besides altered calcium homeostasis through the membrane and increased number of weaker regenerating fibres, which can give rise to fundamental features of the dystrophic process, common to other MDs, such as the intrinsic loss

of contractile strength of muscle fibres, the preferential involvement of fast fibres and the shift towards a slow muscle phenotype.

Methods

Animals

Mice overexpressing *FRG1* to variable extents under the control of the human skeletal α-actin (HSA) gene promoter were previously generated (Gabellini *et al.* 2006). Briefly, *FRG1* open reading frames were PCR-amplified using the following primer: *FRG1*, HSA-*FRG1*-F 50-GA-TCTAGCGGCCGCCATGGCCGAGTACTCCTATGTGA-AGTCT-300. PCR products were sequenced and cloned into pBSX-HSAvpA, provided by J. Chamberlain. Transgene was excised from agarose gels and purified for microinjection into fertilized eggs recovered from C57BL/6 females crossed with C57BL/6 males. All procedures were performed at the University of Massachusetts Medical School Transgenic Animal Modelling Core Facility. In this work, we used the same three lines of mice we previously characterized (Gabellini *et al.* 2006) in which the transgene was overexpressed at levels within the range previously reported for *FRG1* overexpression in FSHD patients (Gabellini *et al.* 2002): *FRG1*-low, *FRG1*-med, *FRG1*-high. In these lines RT-PCR and Southern blot analysis were used to quantify the *FRG1* expression levels and the transgene copy number (3 for *FRG1*-low, 5 for *FRG1*-med; 9 for *FRG1*-high) which corresponded to 10- (*FRG1*-low), 30- (*FRG1*-med), and 50-fold (*FRG1*-high) over the endogenous level of the murine *FRG1* gene (Gabellini *et al.* 2006).

This study was carried out on female *FRG1* transgenic mice at 12 weeks of age; C57bL/6 mice of matched age served as controls. Animals were initially housed in the animal house facility of the Program in Gene Function and expression of the University of Massachusetts Medical School, under the care of the Department of Animal Medicine. At the age of 8 weeks mice were shipped (World Courier) to Italy avoiding extreme temperature during transportation. Once in Italy animals were individually housed in the animal house facility of the Department of Experimental Medicine (University of Pavia, Italy), maintained on a 12 : 12 h light–dark cycle and given unlimited access to food (Dottori Piccioni Italy) and water for the duration of the study. On the day of the experiment, the animals were weighed and killed by cervical dislocation. Muscles (facials: masseter; respiratory: intercostals and diaphragm; anterior limbs: deltoids, biceps and triceps; posterior limbs: soleus, tibialis, vastus and gastrocnemius) were carefully dissected under a stereomicroscope, blotted on filter paper, weighed and stored for analysis. The experimental protocols were approved by the Animal Ethics Committee of the University of Pavia.

Morphological analysis

Muscle samples were included in OCT (Tissue-tek) embedding medium, frozen in liquid nitrogen and serial transverse sections (8 μm thick) were cut using a Leica CM 1850 cryostat. Sections were used for haematoxylin-eosin (H&E) staining, according to standard procedures (Gabellini *et al.* 2006). The percentage of centrally nucleated fibres was calculated in non-consecutive sections (at least five for each muscle) as (number of centrally nucleated fibres/total number of fibres considered) $\times$ 100 (no less than 600 for each group of mice, $n = 5$).

Analysis of force and velocity of single muscle fibres

Absolute (Po) and specific force (Po over the fibre cross-sectional area, Po/CSA) of single muscle fibres were measured in skinned preparations using an approach routinely used for years in our laboratory. All the procedures used have been previously described in detail (Bottinelli *et al.* 1991, 1996; D'Antona *et al.* 2006) except for the solutions which were modified. The skinning solution previously described (D'Antona *et al.* 2006) (150 mM potassium propionate, 5 mM KH_2PO_4, 5 mM magnesium acetate, 3 mM Na_2ATP, 5 mM EGTA, pCa 9.0) was enriched with protease inhibitors (leupeptin 20 μM and E-64 10 μM). Pre-activating (PA) and activating (A) solutions had the following composition: PA: imidazole-propionate 10 mM, magnesium propionate 2.5 mM, potassium propionate 170 mM, K_2-EGTA 5 mM; A: Imid-p 10 mM, magnesium propionate 2.2 mM, potassium phosphate 170 mM, K_2-EGTA 0.11 mM, Ca-EGTA 4.8 mM. In both solutions, Na_2ATP 5 mM and protease inhibitors leupeptin and E-64 were added. Ionic strength was 200 mM in all solutions. The pH of all solutions was set at 7.0.

Po was determined at pCa 4.5, 12°C and optimal sarcomeric length for force developing (2.5 μm) (Pellegrino *et al.* 2003). Po/CSA was expressed as $kN\ m^{-2}$.

The set-up for single muscle fibre analysis was located on the stage of an inverted microscope which enabled us to view the specimen at $\times$320 magnification. CSA was determined, assuming a circular shape, from the mean of three diameters without correction for the swelling which is know to occur in demembranated specimens (Godt & Maughan, 1977). As discussed before (D'Antona *et al.* 2006), skeletal muscle fibres do not always have a circular cross-section and, due to the procedure used to mount the fibre in the set-up, only the largest of the two main diameters could be routinely measured. Therefore, an overestimation of CSA could occur and the degree of overestimation was bound to depend on the shape of the cross-section. To make sure that variation in the shape of the cross-section between WT and dystrophic fibres did not introduce a systematic error in the determination

of CSA and affect the reliability of Po/CSA comparisons we used a procedure previously described (D'Antona *et al.* 2006). Briefly, immediately after dissection, muscles were frozen in liquid nitrogen for subsequent histological analysis. On such sections the larger and smaller diameter of a large population of muscle fibres from WT and *FRG1*-high mice were determined using freely available image analysis software (Scion Image, Scion Corp., USA). CSA was determined either using the largest diameter and assuming a circular shape or using both the largest and the smallest diameters and considering an elliptical shape for both WT and *FRG1*-med fibres. The ratio between the measurement based on a circular shape and the measurement based on an elliptical shape was not significantly different among WT (1.23 ± 0.05 $n = 40$ from 4 mice), *FRG1*-low (1.21 ± 0.07 $n = 40$) and *FRG1*-med (1.32 ± 0.06 $n = 40$ from 4 mice) fibres. As expected, the CSA determination assuming a circular shape somewhat underestimated Po/CSA, but could not introduce any systematic error in the comparison of Po/CSA (D'Antona *et al.* 2006).

To determine maximum shortening velocity (V_o), the slack test technique was employed (Bottinelli *et al.* 1996); V_o was expressed as fibre lengths per second ($L\,s^{-1}$). In skinned fibres, disorder of the striation pattern can occur during maximal activation and this might affect determination of V_o. To ensure that specimens did not go through any significant sarcomere disorganization: (i) muscle fibres were viewed before, during and after each activation at $\times 320$ and were discarded if non-uniformities were seen; (ii) fibres which went through a force loss of more than 10% between the first and the last (fifth–sixth) activation used to determine V_o were discarded even in the absence of clear non-uniformities. Indeed, as the fibre segments used for functional analysis were kept short (~ 1.0 mm), were chosen on the basis of uniform CSA and were quickly and uniformly activated using a previously described procedure (Bottinelli *et al.* 1994), few fibres did not pass the quality controls and had to be discarded. The slack test manoeuvres enable us to determine the series compliance. As expected, series compliance ranged between 3.0% and 5.5% with no significant differences between corresponding fibre types of WT and FSHD mice.

At the end of the mechanical experiment, fibres were put in 20 μl of Leammli buffer (Laemmli, 1970) and stored at $-20°$C for MHC isoform content analysis.

Fibre typing and myosin isoform identification

The composition in myosin heavy chain (MHC) isoforms was determined in single fibres and in whole muscles by polyacrylamide-gel electrophoresis on 8% polyacrylamide slab gels after denaturation in sodium dodecyl sulphate (SDS-PAGE) using a procedure previously described

(Bottinelli *et al.* 1994; Pellegrino *et al.* 2003). Four MHC isoforms (MHC-1, MHC-2A, MHC-2X and MHC-2B) could be separated on gels (Pellegrino *et al.* 2003). Single fibres were classified in pure fibre types (type 1, or slow, and type 2A, 2X and 2B or fast) and in hybrid fibre types (type 1–2A, 2AX and 2XB). Densitometric analysis of the MHC bands of whole muscle samples enabled us to assess their MHC isoform distribution (Harridge *et al.* 1996).

Treadmill

On the day of the experiment each mouse was placed on the belt of a six-lane motorized treadmill (Exer 3/6 Treadmill, Columbus Instruments, OH, USA) supplied with shocker plates which could be individually enabled or disabled for each lane. During each test the electrical stimulus was fixed at 200 ms duration, 0.34 mA amplitude and 1 Hz repetition rate. After a 10 min period of acclimation the treadmill was then started at 5 m min^{-1}, 0 deg inclination for 5 min. After this period the speed was incrementally increased 1 m min^{-1} every minute until the mouse reached exhaustion. Exhaustion was defined as spending time on the shocker plate without attempting to re-engage the treadmill within 20 s. A video camera (Panasonic, NV-RX10EG) was positioned above the treadmill to record each test on a S-VHS video recorder (Toshiba V-729 W) at 25 frames s^{-1} and video recordings were subsequently used for analysis. The individual and the average time to exhaustion and velocity of running were measured.

Statistical analysis

Data were expressed as means $\pm$ s.e.m., unless otherwise stated. Statistical significance of the differences between means was assessed by ANOVA followed by the Student–Newman–Keuls test or by Student's unpaired t test. A probability of less than 5% was considered significant.

Results

Mice phenotype and function *in vivo*

As expected (Gabellini *et al.* 2006), at 12 weeks, i.e. the age of the mice used for structural and functional analysis, no difference was observed in body weight between *FRG1*-low mice (21.67 ± 0.28 g) and C57bL/6, WT mice (22.33 ± 0.57 g). The *FRG1*-med mice (17.71 ± 2.49 g) were smaller than WT mice, and the *FRG1*-high mice (13.66 ± 1.33 g) were significantly smaller than both WT and *FRG1*-med mice. Table 1 reports the weights of individual muscles of WT and FRG-1 mice. Overall, no signs of muscle atrophy were observed in *FRG1*-low mice, whereas muscle atrophy was clearly present in *FRG1*-med

Table 1. Muscle weights (mg) from controls (WT) and *FRG1* transgenic mice (*FRG1*-low expression; *FRG1*-med expression and *FRG1*-high expression) at 12 week of age (intercostals and masseter are not reported; see text)

District	Muscle	WT	*FRG1*-low	*FRG1*-med	*FRG1*-high
Respiratory	Diaphragm	95 ± 7	104 ± 14	$74 \pm 15^*$	$75 \pm 5^*$
Anterior Limb	Biceps	14 ± 2	14 ± 1	12 ± 3	9 ± 1†
	Triceps	66 ± 2	83 ± 8	$46 \pm 1^*$	$33 \pm 2^*$
Posterior Limb	Soleus	7 ± 0.1	7 ± 0.1	7 ± 0.1	$5 \pm 0.1^*$
	Tibialis	42 ± 4	53 ± 12‡	32 ± 4	$26 \pm 1^*$
	Vastus	111 ± 9	118 ± 9	$61 \pm 19^*$	$48 \pm 11^*$
	Gastrocn.	94 ± 19	108 ± 3	$57 \pm 4^*$	$46 \pm 3^*$

*Significantly different from WT and *FRG1*-low; †significantly different from WT, *FRG1*-low and *FRG1*-med; ‡significantly different from WT and *FRG1*-med. Means ± S.D. $P < 0.05$, $n = 5$.

and *FRG1*-high, consistent with what has been previously observed (Gabellini *et al.* 2006).

At the same age, tolerance to exercise, as evidenced in an incremental treadmill test to exhaustion (see Methods), was also in line with our previous observations (Gabellini *et al.* 2006), being significantly lower in *FRG1*-high (10.70 ± 1.57 min) and *FRG1*-med (13.50 ± 3.41 min) than in WT (20.80 ± 6.42 min). *FRG1*-low mice (22.30 ± 5.29 min) were not different from WT mice also in this respect.

As largely expected, the genotypic analysis and the above data confirm that the three lines of mice overexpressing *FRG1* previously generated (Gabellini *et al.* 2006) and used in the present study maintained the same characteristics.

Contractile properties of single muscle fibres

A large population ($n = 329$) of single muscle fibres were dissected from the gastrocnemius and soleus muscles of WT, *FRG1*-low and *FRG1*-med mice at 12 weeks of age ($n = 10$). *FRG1*-high mice were not included in this study as the severity of the disease precluded dissection of large populations of well preserved individual muscle fibres. The mean values of cross-sectional area (CSA), specific force, and maximum shortening velocity and tension deficit of the single muscle fibres analysed were reported in Fig. 1. Interestingly, type 1 and type 2A single muscle fibres not only from FRG1-med, but also from FRG1-low mice, which did not show any clear phenotypic sign of MD and whose muscles were not smaller than WT, were smaller than corresponding fibre types of WT mice.

Figure 1*B* shows the mean values of Po/CSA of the same fibres reported in Fig. 1*A*. Types 2X and 2B fibres from both *FRG1*-low and *FRG1*-med transgenic mice were significantly weaker than those from WT animals, whereas type 2A fibres were significantly weaker only in *FRG1*-med transgenic mice. Although a trend towards a lower isometric force of type 1 fibres was reported in both *FRG1*-low and *FRG1*-med, it did not reach statistical significance. To more readily compare the impairment in

strength of the different fibre types, the force deficit, i.e. force *FRG1*/force WT $\times$ 100 was calculated for each fibre type and reported in Fig. 1*D*. Force deficit increased in the order type 1 $\rightarrow$ 2A $\rightarrow$ 2X $\rightarrow$ 2B fibres. The latter results indicate that fast muscle fibres, and especially the fastest type 2B fibres, were preferentially involved in the dystrophic process.

Unloaded shortening velocity (V_o) was also impaired in dystrophic fibres. With the exception of type 2X and 2B fibres from *FRG1*-low, all fibre types of both FRG1 lines analysed (low and med) had lower Vo than corresponding fibre type of WT mice (Fig. 1*C*).

Alterations of single muscle fibre properties, being observed in FRG1-low mice that did not show clear manifestations of MD (body weight loss, muscle atrophy, decrease in exercise tolerance) can be considered early signs of MD.

Myosin heavy chain isoform distribution of *FRG1* mice muscles

The distribution of MHC isoforms, a widely used index of fibre type distribution, was determined in 10 muscles (facials: masseter; respiratory: intercostals and diaphragm; upper limbs: deltoids, biceps and triceps; lower limbs: soleus, tibialis, vastus and gastrocnemius) of WT and *FRG1*-med mice by densitometric analysis of MHC bands separated by SDS-PAGE (Table 2). Consistent with the observation that type 1, slow fibres were relatively spared by the dystrophic process whereas type 2B fibres were the most affected fibre type, *FRG1*-med mice showed a significant shift towards the expression of slower MHC isoforms in all muscles studied.

In masseter the shift was from MHC-2B and 2X towards 2A, in intercostals and deltoid from MHC-2B towards MHC-2X and 2A; in diaphragm the shift was from MHC-2B, 2X and 2A towards MHC-1. As regards anterior and posterior limb muscles, in biceps, triceps, vastus and gastrocnemius the shift was from MHC-2B towards

Table 2. Myosin heavy chain (MHC) composition (%) of muscles from controls (WT) and *FRG1*-med transgenic mice at 12 week of age

District	Muscle	MHC-1 (%)		MHC-2A (%)		MHC-2X (%)		MHC-2B (%)	
		WT	*FRG1*-m	WT	*FRG1*-m	WT	*FRG1*-m	WT	*FRG1*-m
Facial	Masseter	4.7 ± 5.5	9.3 ± 10.4	0 ± 0	16.1 ± 17.7*	77.3 ± 8.0	68.9 ± 5.7*	17.9 ± 12.6	5.7 ± 6.1*
Respiratory	Diaphragm	11.6 ± 2.5	15.7 ± 0.8*	39.5 ± 0.5	54.7 ± 2.0*	37.7 ± 3.9	27.7 ± 2.3*	11.1 ± 1.9	1.8 ± 0.7*
	Intercostal	6.1 ± 2.3	11.9 ± 1.8*	17.3 ± 3.2	24.7 ± 3.9*	19.9 ± 4.3	33 ± 1.5*	56.7 ± 2.3	30.3 ± 3.7*
Anterior limb	Deltoid	11.6 ± 1.2	13.0 ± 2.2	8.0 ± 1.2	15.7 ± 1.4*	14.0 ± 1.2	21.0 ± 1.5*	66.4 ± 0.6	50.2 ± 4.7*
	Biceps	0 ± 0	0 ± 0	16.1 ± 2.9	27.2 ± 0.5*	24.7 ± 1.3	27.2 ± 1.0*	58.4 ± 4.8	45.8 ± 1.2*
	Triceps	0 ± 0	28.7 ± 3.0*	18.2 ± 1.9*	0 ± 0	23.5 ± 2.9	27.6 ± 3.1*	58.2 ± 3.7	45.7 ± 4.2*
Posterior limb	Soleus	37.1 ± 1.3	64.1 ± 3.5*	51.5 ± 5.5	27.6 ± 3.6*	11.4 ± 4.7	8.2 ± 2.1*	0 ± 0	0 ± 0
	Tibialis	0 ± 0	9.7 ± 10.4*	5.4 ± 7.4	7.4.9 ± 8.0*	21.9 ± 2.0	27.8 ± 4.8*	72.7 ± 4.2	55.1 ± 22.*
	Vastus	0 ± 0	2.3 ± 0.3*	6.8 ± 1.9	17.0 ± 0.8*	11.1 ± 2.0	28.7 ± 0.5*	82.1 ± 1.3	52.0 ± 1.3*
	Gastrocn.	0 ± 0	24.2 ± 2.2*	7.3 ± 7.9	11.4 ± 12.3	16.1 ± 2.4	23.7 ± 2.7*	76.6 ± 6.8	52.1 ± 3.5*

*Significantly different from correspondent isoforms. Means ± s.d. $P < 0.05$, $n = 10$.

MHC-1; finally in soleus the shift was from MHC-2X and especially MHC-2A towards MHC-1 (Table 2).

To clarify whether a shift of muscle phenotype could be considered an early sign of FSHD, the MHC isoform distribution of soleus, as an example of a slow, mildly affected muscle, and of biceps and vastus (Fig. 2) as examples of fast significantly affected muscles was studied in all lines of *FRG1* mice. Interestingly the overall shift
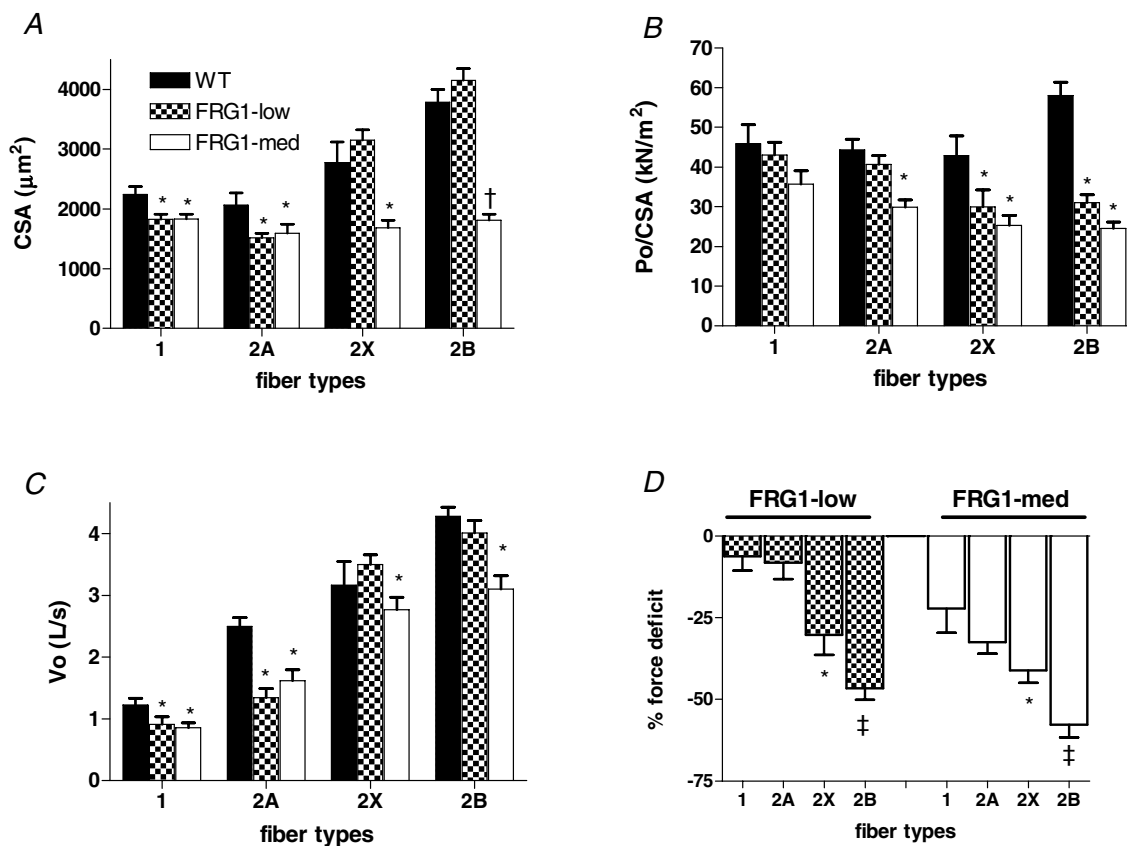

Figure 1. Cross-sectional area (CSA, *A*), specific force (Po/CSA, *B*), maximum shortening velocity (V_o, *C*) and tension deficit ((*FRG1*/force of WT) × 100, *D*) of single muscle fibres from WT, *FRG1*-low and *FRG1*-med mice

All fibres ($n = 329$) were identified on the basis of MHC isoforms content determined by SDS-PAGE in pure type 1, 2A and 2B. CSA is expressed in μm, Po/CSA in kN m^{-1}, V_o in length per second (L s^{-1}) and force deficit as percentage force loss of corresponding fibres from WT mice. The height of each bar represents the mean (± s.e.m.). *Significantly different from corresponding fibres type of WT; †significantly different from corresponding fibres of WT and *FRG1*-low; ‡significantly different from type 1 and type 2A; #significantly different from type 1, 2A and 2X; $P < 0.05$ $n = 10$.
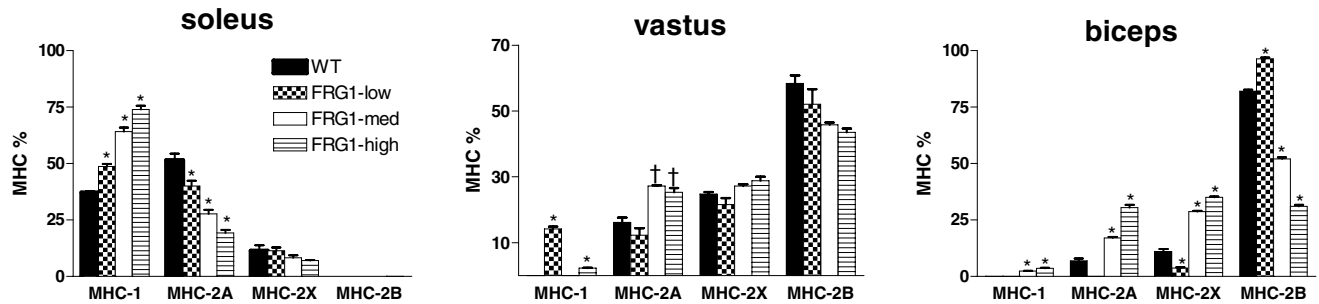
Figure 2. Myosin heavy chain (MHC) distribution of soleus, vastus and biceps in WT, *FRG1*-low, *FRG1*-med and *FRG1*-high mice

MHC distribution determined from muscle samples (*n* = 5) of the four groups of mice by SDS-PAGE separation followed by densitometric analysis of MHC bands. The height of each bar represents the mean (± s.e.m.). *Significantly different from the other groups; †significantly different from WT and *FRG1*-low; $P < 0.05$, $n = 5$.

towards a slower phenotype appeared evident in all muscles analysed and in all lines, even in soleus muscles (Fig. 2) of *FRG1*-low mice which did not show clear histological signs of MD (Fig. 3). Thus, change in MHC composition of the muscle can be considered an early sign of the disease.

Muscle morphology of slow and fast muscles

The observation that the dystrophic process preferentially affected size and function of the fastest fibre type (2B)

and relatively spared the slowest fibre type (1) should be reflected not only in a fast to slow transition in fibre type composition of the muscles, but also in a differential dystrophic deterioration of fast and slow muscle. To clarify whether this was actually the case, the morphology of the muscles, the ratio between muscle weight and body weight and the percentage of centrally nucleated fibres were compared through muscles and FRG-1 lines.

As expected (Gabellini *et al.* 2006), dystrophic histological features, namely fibre necrosis, number of centrally nucleated fibres, connective tissue, and
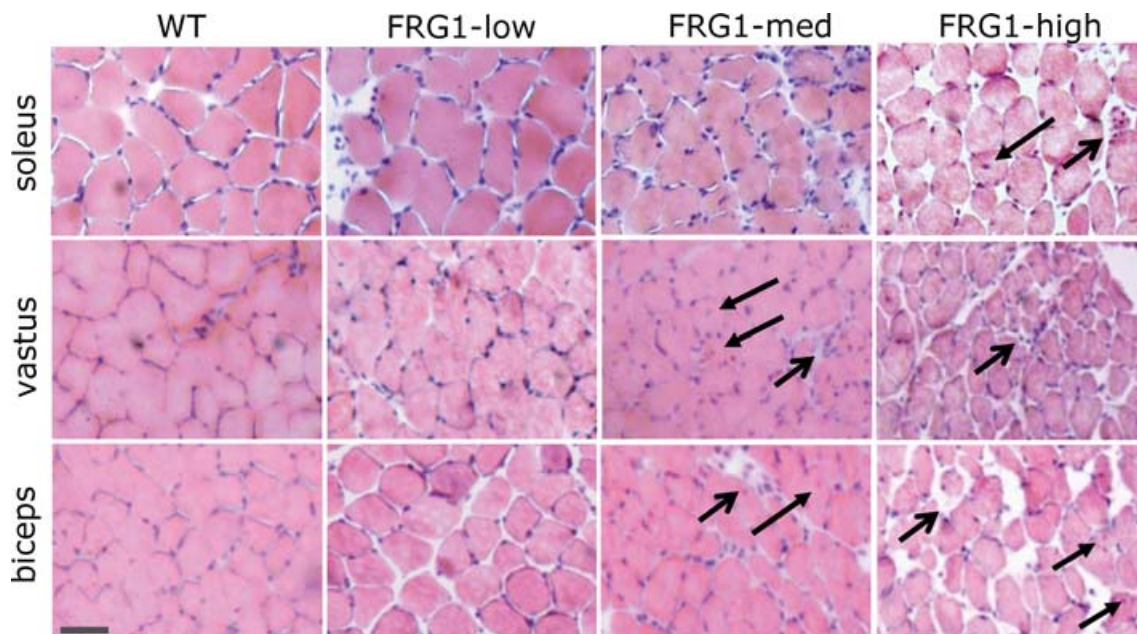

Figure 3. Heamatoxilyn–eosin stained sections from soleus, vastus and biceps muscle of WT, *FRG1*-low, *FRG1*-med and *FRG1*-high mice

Distribution of muscle damage appeared to depend on the muscle considered and on the level of *FRG1* expression. In all muscles no clear histological signs of muscular dystrophy were detectable in *FRG1*-low mice, whereas signs of fibre degeneration and necrosis (open arrows) as well as centrally nucleated fibres (close arrows) were detectable in biceps and vastus from *FRG1*-med and *FRG1*-high mice and appeared to be more evident in *FRG1*-high than *FRG1*-med mice. Bar represents 30 μm.
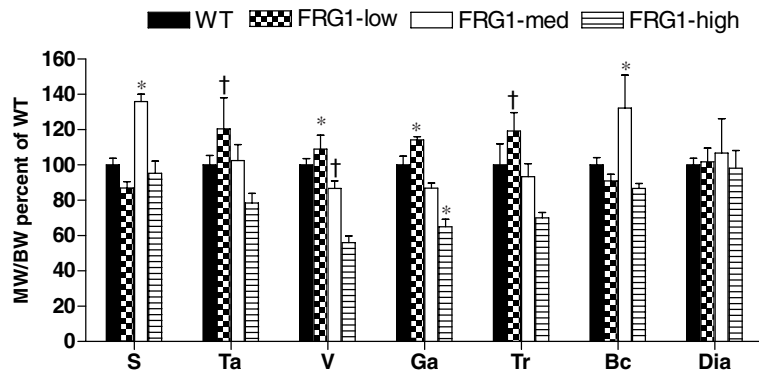
increased fibre size variability were found to depend on *FRG1* expression levels being almost absent in muscles of *FRG1*-low mice and increasingly more evident in *FRG1*-med and *FRG1*-high. More interestingly, soleus appeared much more spared by the disease process than vastus and biceps (Fig. 3).

To compare the degree of atrophy of different muscles, the ratio between muscle weight (MW) and body weight (BW) was determined and expressed relative to the MW/BW ratio of the same muscle of age-matched WT mice (Fig. 4). The MW/BW ratio of soleus (relatively spared by the disease process) was not smaller in *FRG1*-low and *FRG1*-high mice than in WT mice and larger in *FRG1*-med than in WT, suggesting compensatory hypertrophy. In *FRG1*-high apart from soleus and diaphragm all other muscles analysed showed significantly lower BW/MW ratio in comparison with WT mice. *FRG1*-med showed somewhat lower values and *FRG1*-low somewhat higher values than WT, but the difference did not reach statistical significance (Fig. 4). Some of the muscles (masseter, intercostals) were not included in the analysis of MW (Table 1) and MW/BW as their shape and architecture did not enable us to determine their weight consistently through experimental groups.
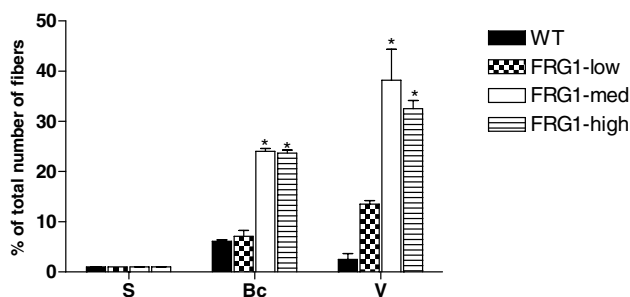
The degree of involvement of soleus, vastus and biceps was also quantified by determining the percentage of centrally nucleated fibres, considered an index of muscle fibre regeneration (Ferrari *et al.* 1998). Figure 5 shows that in soleus the percentage of centrally nucleated fibres was very similar in WT and in all *FRG1* lines, whereas biceps and vastus had a highly significant increase of centrally nucleated fibres in all *FRG1*-med and *FRG1*-high in comparison with WT. In *FRG1*-low a significant increase of centrally nucleated fibres, but lower than in *FRG1*-med and high, was only observed in vastus.

Discussion

The present work studied structure and function of muscle fibres in a murine model of MD in which the pathogenesis of the disease cannot be initially traced back to a membrane defect. The main results indicate that: (i) muscle fibres are intrinsically weaker in the FSHD mice, and their loss of strength is an early sign of MD; (ii) fast muscle fibres are preferentially involved in the dystrophic process; (iii) the latter phenomenon can be a major determinant of the slower muscle phenotype of dystrophic muscles and can play a role in the differential distribution of the disease among muscles of the same animal.

Figure 5. Percentage of centrally nucleated fibres in soleus (S), biceps (Bc) and vastus (V) of WT, *FRG1*-low, *FRG1*-med and *FRG1*-high mice
At least 600 fibres were analysed from each group of mice ($n = 5$). The height of each bar represents the mean (± S.E.M.). *Significantly different from WT and *FRG1*- low, $P < 0.05$, $n = 10$.

Muscle weakness in MDs is not only due to a loss of contractile muscle mass

In the mouse model of FSHD, impaired mobility was ascribed to muscle atrophy (quantitative mechanism) which was observed at early stages of the disease in the absence of any, even transient, significant compensatory hypertrophy (Gabellini *et al.* 2006). The present findings, showing a loss of specific force (Po/CSA) of single muscle fibres, indicate the existence of a qualitative mechanism of muscle weakness based on a loss of intrinsic contractile strength. As type 2B fibres, which are the most represented fibre type in mice muscles (Pellegrino *et al.* 2003), lose approximately half of their intrinsic strength even in *FRG1*-low mice, the latter mechanism can play a major

role, together with a loss of muscle mass, in determining muscle weakness in the FSHD mice *in vivo*. As muscle weakness *in vivo*, the loss of specific force of muscle fibres appeared related to the progression of the disease being more evident in *FRG1*-med than in *FRG1*-low mice.

The results obtained in this work confirm and extend previous findings. Earlier studies showed a loss of specific force in some population of skinned muscle fibres in *mdx* mice (Williams *et al.* 1993) and in an earlier murine model of MD, 129ReJ mice (Fink *et al.* 1986). Very recently, we consistently showed a loss of specific force in the fastest type 2B fibre type in several mouse models of MDs: *mdx* mice (Denti *et al.* 2006), α-sarcoglycan KO mice (Sampaolesi *et al.* 2003), scid-*mdx* mice (Torrente *et al.* 2004). It appears that the intrinsic loss of contractile strength is a major mechanism underlying muscle weakness in MD. Moreover, the latter phenomenon could be a fundamental feature of the dystrophic process as it is common to MDs having different pathogenetic mechanism and it is an early manifestation of the disease, at least in the only model, the FSHD mice, in which specific force deficit could be related to the severity of the disease.

The loss in specific force of muscle fibres observed in recent studies on *mdx* mice (Denti *et al.* 2006) is not in agreement with some earlier findings on the same mouse model (Takagi *et al.* 1992; Lynch *et al.* 2000). The dependence of muscle fibre alterations on fibre type and on the progression of the disease suggests possible causes for such discrepancy. In fact, in earlier works, muscle fibres were not precisely typed and results might have been affected by pooling and comparing muscle fibres of different types and therefore differentially affected by the disease.

Mechanisms underlying the loss of specific force are still unclear. Interestingly, the loss of Po/CSA in atrophic muscle fibres of elderly sedentary and immobilized humans has been shown to be linearly related to a decrease in myosin concentration within the fibres (Hook *et al.* 2001; D'Antona *et al.* 2003; D'Antona *et al.* 2006). As in MDs the balance between myofibrillar protein synthesis and degradation is shifted towards degradation (McKeran *et al.* 1977; Elia *et al.* 1981; Warnes *et al.* 1981), the latter phenomenon might be involved in MDs as well. Moreover a possible contribution to reduced specific force generation may also arise from increased number of weaker regenerating fibres which, in the presence of degeneration–regeneration cycles, initially replace necrotic fibres (Gregorevic *et al.* 2004). Nevertheless in *FRG1* mice the observation of a limited amount of necrosis and regeneration, even in *FRG1*-high mice, suggests that this mechanism might play a minor role.

The observation that dystrophic fibres have not only lower specific force (Po/CSA), but also lower unloaded shortening velocity (V_o) than WT fibres is relevant as it can provide an additional explanation of muscle weakness and altered motility of FSHD mice. During movement and locomotion *in vivo*, muscles shorten against a load developing power (i.e. force times velocity). A loss of both Po/CSA and shortening velocity is bound to determine a much higher loss of mechanical power of the muscles and consequently a much more evident limitation of motility than a loss of force *per se*. It is unclear, whether a loss of V_o is a common features of all mouse models of MD as most studies so far focused on force. Recently it has been shown that diaphragm strips from *mdx* mice shorten at lower velocity than diaphragm strips from controls (Coirault *et al.* 1999). The origin of such impairment is unclear. In light of the modulator role played by myosin light chain (MLC) isoforms on V_o (Bottinelli *et al.* 1994), it might be due to a MD coupled shift in MLC composition of muscle fibres. However, it has been shown that V_o of muscle fibres and isolated myosin can change without a significant change in MLC content (Hook *et al.* 2001; D'Antona *et al.* 2003, 2006) possibly due post-translational modifications of the myosin molecule (Ramamurthy *et al.* 2001).

Fast muscle fibres are preferentially involved in the dystrophic process

An early morphological analysis of muscle fibres of patients affected by Duchenne MD (Webster *et al.* 1988) gave rise to the strong belief that the dystrophic process preferentially strikes fast fibres. The observation of a lower stretch-induced damage in slow (soleus) than in fast (EDL) muscles of *mdx* mice (Moens *et al.* 1993; Consolino & Brooks, 2004) supported such belief. However, no systematic comparative analysis of specific force of identified types of dystrophic fibres had been performed so far. The only data available suggested a significant force loss in slow muscle fibres from soleus, but not in fast muscle fibres from EDL muscles of *mdx* mice (Williams *et al.* 1993).

In this work, muscle fibres have been precisely identified on the basis of MHC isoform content, and contractile properties of three of the four types of muscle fibres expressed in skeletal muscle of the mice have been compared. The results indicate that in the FSHD mice the loss of specific force is significantly more evident in type 2B than in type 1, slow fibres (type 2A and 2X fibres being intermediate). Such findings support the general belief of a preferential involvement of fast fibres in the dystrophic process. Moreover, being observed in a murine model of MD with very peculiar pathogenetic features, the phenomenon appears a common feature of most MDs, regardless the underlying genetic defect.

The preferential involvement of the fastest fibre types in the dystrophic process is consistent with several concomitant findings. The morphological signs of MDs

were less evident in soleus, the slowest muscle of the mice (45% MHC-1) than in fast muscles such as the biceps (27% MHC-2X and 46% MHC-2B) and the vastus (11% MHC-2X and 82% MHC-2B). MHC isoform distribution of a large population of skeletal muscles was shifted from faster to slower isoforms. The percentage of centrally nucleated fibres was normal in soleus and diaphragm (15% MHC-1 and 40% MHC-2A), but was much higher in fast muscle such as the vastus and the biceps.

In *FRG1* mice a possible contribution to the observed selective involvement of fast fibres and fast muscles may take place from higher susceptibility of such fibres and muscles to eccentric contraction-induced damage as previously observed in *mdx* mice (Moens *et al.* 1993; Raymackers *et al.* 2003; Yeung *et al.* 2003). Indeed, the preferential deterioration of the fastest fibre types could be a one of the major determinants of the latter features common to most MDs.

Lack of plasmamembrane defect and muscle fibre deterioration

This study suggests that fundamental features of the dystrophic process are common to the FSHD mice and to the most studied models of MD such as the *mdx* mice and the α-SG-KO mice. The loss of intrinsic strength of muscle fibres (Sampaolesi *et al.* 2003; Torrente *et al.* 2004; Denti *et al.* 2006), the preferential involvement of fast fibres (Webster *et al.* 1988), the fast to slow shift in muscle phenotype (Petrof *et al.* 1993; Muller *et al.* 2001), and the differential involvement of skeletal muscles with soleus being less or later involved in MD (Nguyen *et al.* 2002; Briguet *et al.* 2004) were, in fact, previously observed in *mdx* and, to a certain extent, in α-SG-KO mice. Among the dystrophic features observed, only muscle atrophy is rather distinctive of the FSHD mice (Gabellini *et al.* 2006) and the mouse model of myotonic dystrophy (Mankodi *et al.* 2000; Seznec *et al.* 2001). Pseudo-hypertrophy is mostly observed, in fact, in the other mouse models (Watchko *et al.* 2002).

In the FSHD mice we previously demonstrated sarcolemmal integrity based on lack of Evans blue uptake by muscle fibres, normal creatine kinase serum levels and integrity of the DCG complex (Gabellini *et al.* 2006). This feature is common to other murine models of MDs, as calpain-3 deficiency, which also fails to show a clear increase in serum creatine kinase (Richard *et al.* 2000) and Evans blue uptake (Fougerousse *et al.* 2003). On the contrary a consistent increase of creatine kinase serum levels and the appearance of Evans blue positive cells are considered distinctive features in animal models of MDs due to alterations of the DCG complex (Sampaolesi *et al.* 2003; Denti *et al.* 2006).

In *FRG1* mice, lack of obvious sarcolemmal impairment appeared in contrast with the observation of unspecific

signs of fibre degeneration–regeneration. The extent of unspecific histopathological signs of MD correlated with *FRG1* overexpression but appeared somehow moderate relative to *mdx* or α-SG-KO mice (Sampaolesi *et al.* 2003; Denti *et al.* 2006). In particular quantification of the number of centrally nucleated fibres showed, in all muscles analysed, a moderate level of central nuclei in *FRG1* transgenic mice relative to *mdx* and α-SG-KO even in the presence of *FRG1*-high expression (Gabellini *et al.* 2006). Furthermore no regenerating myosins (neonatal or developmental MyHCs) have been detected in all *FRG1* lines thus suggesting a low level of muscle degeneration–regeneration.

Nevertheless coexistence of unspecific dystrophic changes and sarcolemmal integrity does not represent a unique feature of the *FRG1* mouse and FSHD as it has been already found in the mouse model of myotonic dystrophy (Mankodi *et al.* 2000; Seznec *et al.* 2001) and myotonic dystrophy (Casanova & Jerusalem, 1979).

Overall sarcolemmal integrity in *FRG1*-mice suggests that the dystrophic features observed so far cannot be ascribed to an obvious change of calcium levels followed by activation of proteolysis as in MDs due to alteration of DGC (Allen *et al.* 2005; Deconinck & Dan, 2007). Nevertheless no data on extracellular and intracellular calcium levels are currently available for *FRG1*-mice and the possible contribution of altered calcium homeostasis in determining the observed histological changes should be investigated.

Furthermore the present findings strongly suggest that fundamental features of the dystrophic process very similar to those observed in presence of DCG alterations can be the common outcome of alternative pathogenetic mechanisms. Such fundamental manifestations (loss of specific force, preferential involvement of fast muscle fibres, fast to slow shift in muscle phenotype, differential involvement of muscles) occur at early stages of the disease at least in the FSHD mice whereas histopathological signs of MD increase with age (Gabellini *et al.* 2006). Therefore, it can be ruled out that they are common in different MDs just because they necessarily appear in any heavily compromised muscle whatever the underlying myopathic process.

The physiological role of *FRG1* and the mechanism by which *FRG1* overexpression leads to the myopathic response are largely obscure. *FRG1* is a nuclear protein identified as a component of purified spliceosomes (Rappsilber *et al.* 2002). We found that *FRG1* over-expression is responsible for abnormal alternative splicing of specific pre-mRNAs and this can play a major role in the pathogenesis of FSHD (Gabellini *et al.* 2006). In particular it is likely that both in *FRG1* mice and FSHD patients the increased levels of aberrant proteins may contribute to the histopathological features arising.

Interestingly abnormal mRNA processing plays a pathogenetic role in other neuromuscular disorders such as oculopharyngeal muscular dystrophy (Calado *et al.* 2000) and myotonic MD (Ranum & Day, 2004) and a recent study on muscle fibres of patients affected by myotonic MD (Krivickas *et al.* 2000) showed a loss of specific force, although limited to slow fibres. The latter observation strengthens the idea that abnormal mRNA processing can determine the structural and functional alterations at the fibre level. However the causal link between aberrant pre-mRNA processing and loss in force of dystrophic fibres is still unknown.

In conclusion, the analysis of the FSHD mice provided a detailed characterization of a novel mouse model of a major human MD which is bound to be used to further study both the pathogenesis and the therapy of such important disease. Moreover, the observation that fundamental features of the dystrophic process are common to the FSHD mice and to the most studied murine models of MD strongly suggest they can be on a common path of different pathogenetic mechanisms.

References

Allen DG, Whitehead NP & Yeung EW (2005). Mechanisms of stretch-induced muscle damage in normal and dystrophic muscle: role of ionic changes. *J Physiol* **567**, 723–735.

Bonaldo P, Braghetta P, Zanetti M, Piccolo S, Volpin D & Bressan GM (1998). Collagen VI deficiency induces early onset myopathy in the mouse: an animal model for Bethlem myopathy. *Hum Mol Genet* **7**, 2135–2140.

Bottinelli R, Betto R, Schiaffino S & Reggiani C (1994). Unloaded shortening velocity and myosin heavy chain and alkali light chain isoform composition in rat skeletal muscle fibres. *J Physiol* **478**, 341–349.

Bottinelli R, Canepari M, Pellegrino MA & Reggiani C (1996). Force-velocity properties of human skeletal muscle fibres: myosin heavy chain isoform and temperature dependence. *J Physiol* **495**, 573–586.

Bottinelli R, Schiaffino S & Reggiani C (1991). Force-velocity relations and myosin heavy chain isoform compositions of skinned fibres from rat skeletal muscle. *J Physiol* **437**, 655–672.

Briguet A, Courdier-Fruh I, Foster M, Meier T & Magyar JP (2004). Histological parameters for the quantitative assessment of muscular dystrophy in the mdx-mouse. *Neuromuscul Disord* **14**, 675–682.

Calado A, Tome FM, Brais B, Rouleau GA, Kuhn U, Wahle E & Carmo-Fonseca M (2000). Nuclear inclusions in oculopharyngeal muscular dystrophy consist of poly(A) binding protein 2 aggregates which sequester poly(A) RNA. *Hum Mol Genet* **9**, 2321–2328.

Casanova G & Jerusalem F (1979). Myopathology of myotonic dystrophy. A morphometric study. *Acta Neuropathol (Berl)* **45**, 231–240.

Coirault C, Lambert F, Marchand-Adam S, Attal P, Chemla D & Lecarpentier Y (1999). Myosin molecular motor dysfunction in dystrophic mouse diaphragm. *Am J Physiol Cell Physiol* **277**, C1170–C1176.

Consolino CM & Brooks SV (2004). Susceptibility to sarcomere injury induced by single stretches of maximally activated muscles of mdx mice. *J Appl Physiol* **96**, 633–638.

D'Antona G, Lanfranconi F, Pellegrino MA, Brocca L, Adami R, Rossi R, Moro G, Miotti D, Canepari M & Bottinelli R (2006). Skeletal muscle hypertrophy and structure and function of skeletal muscle fibres in male body builders. *J Physiol* **570**, 611–627.

D'Antona G, Pellegrino MA, Adami R, Rossi R, Carlizzi CN, Canepari M, Saltin B & Bottinelli R (2003). The effect of ageing and immobilization on structure and function of human skeletal muscle fibres. *J Physiol* **552**, 499–511.

Deconinck N & Dan B (2007). Pathophysiology of duchenne muscular dystrophy: current hypotheses. *Pediatric Neurol* **36**, 1–7.

Denti MA, Rosa A, D'Antona G, Sthandier O, De Angelis FG, Nicoletti C, Allocca M, Pansarasa O, Parente V, Musaro A, Auricchio A, Bottinelli R & Bozzoni I (2006). Body-wide gene therapy of Duchenne muscular dystrophy in the mdx mouse model. *Proc Natl Acad Sci U S A* **103**, 3758–3763.

Durbeej M & Campbell KP (2002). Muscular dystrophies involving the dystrophin-glycoprotein complex: an overview of current mouse models. *Curr Opin Genet Dev* **12**, 349–361.

Elia M, Carter A, Bacon S, Winearls CG & Smith R (1981). Clinical usefulness of urinary 3-methylhistidine excretion in indicating muscle protein breakdown. *Br Med J (Clin Res Ed)* **282**, 351–354.

Ferrari G, Cusella-De Angelis G, Coletta M, Paolucci E, Stornaiuolo A, Cossu G & Mavilio F (1998). Muscle regeneration by bone marrow-derived myogenic progenitors. *Science* **279**, 1528–1530.

Fink RH, Stephenson DG & Williams DA (1986). Calcium and strontium activation of single skinned muscle fibres of normal and dystrophic mice. *J Physiol* **373**, 513–525.

Fink RH, Stephenson DG & Williams DA (1990). Physiological properties of skinned fibres from normal and dystrophic (Duchenne) human muscle activated by Ca^{2+} and Sr^{2+}. *J Physiol* **420**, 337–353.

Fougerousse F, Gonin P, Durand M, Richard I & Raymackers JM (2003). Force impairment in calpain 3-deficient mice is not correlated with mechanical disruption. *Muscle Nerve* **27**, 616–623.

Gabellini D, D'Antona G, Moggio M, Prelle A, Zecca C, Adami R, Angeletti B, Ciscato P, Pellegrino MA, Bottinelli R, Green MR & Tupler R (2006). Facioscapulohumeral muscular dystrophy in mice overexpressing FRG1. *Nature* **439**, 973–977.

Gabellini D, Green MR & Tupler R (2002). Inappropriate gene activation in FSHD: a repressor complex binds a chromosomal repeat deleted in dystrophic muscle. *Cell* **110**, 339–348.

Gillis JM (1999). Understanding dystrophinopathies: an inventory of the structural and functional consequences of the absence of dystrophin in muscles of the mdx mouse. *J Muscle Res Cell Motil* **20**, 605–625.

Godt RE & Maughan DW (1977). Swelling of skinned muscle fibers of the frog. Experimental observations. *Biophys J* **19**, 103–116.

Gregorevic P, Plant DR, Stupka N & Lynch GS (2004). Changes in contractile activation characteristics of rat fast and slow skeletal muscle fibres during regeneration. *J Physiol* **558**, 549–560.

Harridge SD, Bottinelli R, Canepari M, Pellegrino MA, Reggiani C, Esbjornsson M & Saltin B (1996). Whole-muscle and single-fibre contractile properties and myosin heavy chain isoforms in humans. *Pflugers Arch* **432**, 913–920.

Hook P, Sriramoju V & Larsson L (2001). Effects of aging on actin sliding speed on myosin from single skeletal muscle cells of mice, rats, and humans. *Am J Physiol Cell Physiol* **280**, C782–C788.

Horowits R, Dalakas MC & Podolsky RJ (1990). Single skinned muscle fibers in Duchenne muscular dystrophy generate normal force. *Ann Neurol* **27**, 636–641.

Irwin WA, Bergamin N, Sabatelli P, Reggiani C, Megighian A, Merlini L, Braghetta P, Columbaro M, Volpin D, Bressan GM, Bernardi P & Bonaldo P (2003). Mitochondrial dysfunction and apoptosis in myopathic mice with collagen VI deficiency. *Nat Genet* **35**, 367–371.

Klesert TR, Cho DH, Clark JI, Maylie J, Adelman J, Snider L, Yuen EC, Soriano P & Tapscott SJ (2000). Mice deficient in Six5 develop cataracts: implications for myotonic dystrophy. *Nat Genet* **25**, 105–109.

Krivickas LS, Ansved T, Suh D & Frontera WR (2000). Contractile properties of single muscle fibers in myotonic dystrophy. *Muscle Nerve* **23**, 529–537.

Laemmli UK. (1970). Cleavage of structural proteins during the assembly of the head of bacteriophage T4. *Nature* **227**, 680–685.

Lynch GS, Rafael JA, Chamberlain JS & Faulkner JA (2000). Contraction-induced injury to single permeabilized muscle fibers from mdx, transgenic mdx, and control mice. *Am J Physiol Cell Physiol* **279**, C1290–C1294.

Mankodi A, Logigian E, Callahan L, McClain C, White R, Henderson D, Krym M & Thornton CA (2000). Myotonic dystrophy in transgenic mice expressing an expanded CUG repeat. *Science* **289**, 1769–1773.

McKeran RO, Halliday D & Purkiss P (1977). Increased myofibrillar protein catabolism in Duchenne muscular dystrophy measured by 3-methylhistidine excretion in the urine. *J Neurol Neurosurg Psychiatry* **40**, 979–981.

Moens P, Baatsen PH & Marechal G (1993). Increased susceptibility of EDL muscles from mdx mice to damage induced by contractions with stretch. *J Muscle Res Cell Motil* **14**, 446–451.

Muller J, Vayssiere N, Royuela M, Leger ME, Muller A, Bacou F, Pons F, Hugon G & Mornet D (2001). Comparative evolution of muscular dystrophy in diaphragm, gastrocnemius and masseter muscles from old male mdx mice. *J Muscle Res Cell Motil* **22**, 133–139.

Muntoni F, Brockington M, Torelli S & Brown SC (2004). Defective glycosylation in congenital muscular dystrophies. *Curr Opin Neurol* **17**, 205–209.

Nguyen HH, Jayasinha V, Xia B, Hoyte K & Martin PT (2002). Overexpression of the cytotoxic T cell GalNAc transferase in skeletal muscle inhibits muscular dystrophy in mdx mice. *Proc Natl Acad Sci U S A* **99**, 5616–5621.

Pellegrino MA, Canepari M, Rossi R, D'Antona G, Reggiani C & Bottinelli R (2003). Orthologous myosin isoforms and scaling of shortening velocity with body size in mouse, rat, rabbit and human muscles. *J Physiol* **546**, 677–689.

Petrof BJ, Stedman HH, Shrager JB, Eby J, Sweeney HL & Kelly AM (1993). Adaptations in myosin heavy chain expression and contractile function in dystrophic mouse diaphragm. *Am J Physiol Cell Physiol* **265**, C834–C841.

Ramamurthy B, Hook P, Jones AD & Larsson L (2001). Changes in myosin structure and function in response to glycation. *FASEB J* **15**, 2415–2422.

Ranum LP & Day JW (2004). Myotonic dystrophy. RNA pathogenesis comes into focus. *Am J Human Genet* **74**, 793–804.

Rappsilber J, Ryder U, Lamond AI & Mann M (2002). Large-scale proteomic analysis of the human spliceosome. *Genome Res* **12**, 1231–1245.

Raymackers JM, Debaix H, Colson-Van Schoor M, De Backer F, Tajeddine N, Schwaller B, Gailly P & Gillis JM (2003). Consequence of parvalbumin deficiency in the mdx mouse: histological, biochemical and mechanical phenotype of a new double mutant. *Neuromuscul Disord* **13**, 376–387.

Richard I, Roudaut C, Marchand S, Baghdiguian S, Herasse M, Stockholm D, Ono Y, Suel L, Bourg N, Sorimachi H, Lefranc G, Fardeau M, Sebille A & Beckmann JS (2000). Loss of calpain 3 proteolytic activity leads to muscular dystrophy and to apoptosis-associated IκBα/nuclear factor κB pathway perturbation in mice. *J Cell Biol* **151**, 1583–1590.

Sampaolesi M, Torrente Y, Innocenzi A, Tonlorenzi R, D'Antona G, Pellegrino MA, Barresi R, Bresolin N, De Angelis MG, Campbell KP, Bottinelli R & Cossu G (2003). Cell therapy of α-sarcoglycan null dystrophic mice through intra-arterial delivery of mesoangioblasts. *Science* **301**, 487–492.

Sarkar PS, Appukuttan B, Han J, Ito Y, Ai C, Tsai W, Chai Y, Stout JT & Reddy S (2000). Heterozygous loss of Six5 in mice is sufficient to cause ocular cataracts. *Nat Genet* **25**, 110–114.

Seznec H, Agbulut O, Sergeant N, Savouret C, Ghestem A, Tabti N, Willer JC, Ourth L, Duros C, Brisson E, Fouquet C, Butler-Browne G, Delacourte A, Junien C & Gourdon G (2001). Mice transgenic for the human myotonic dystrophy region with expanded CTG repeats display muscular and brain abnormalities. *Hum Mol Genet* **10**, 2717–2726.

Takagi A, Kojima S, Ida M & Araki M (1992). Increased leakage of calcium ion from the sarcoplasmic reticulum of the mdx mouse. *J Neurol Sci* **110**, 160–164.

Torrente Y, Belicchi M, Sampaolesi M, Pisati F, Meregalli M, D'Antona G, Tonlorenzi R, Porretti L, Gavina M, Mamchaoui K, Pellegrino MA, Furling D, Mouly V, Butler-Browne GS, Bottinelli R, Cossu G & Bresolin N (2004). Human circulating AC133^{+} stem cells restore dystrophin expression and ameliorate function in dystrophic skeletal muscle. *J Clin Invest* **114**, 182–195.

Warnes DM, Tomas FM & Ballard FJ (1981). Increased rates of myofibrillar protein breakdown in muscle-wasting diseases. *Muscle Nerve* **4**, 62–66.

Watchko JF, O'Day TL & Hoffman EP (2002). Functional characteristics of dystrophic skeletal muscle: insights from animal models. *J Appl Physiol* **93**, 407–417.

Webster C, Silberstein L, Hays AP & Blau HM (1988). Fast muscle fibers are preferentially affected in Duchenne muscular dystrophy. *Cell* **52**, 503–513.

Williams DA, Head SI, Lynch GS & Stephenson DG (1993). Contractile properties of skinned muscle fibres from young and adult normal and dystrophic (mdx) mice. *J Physiol* **460**, 51–67.

Yeung EW, Head SI & Allen DG (2003). Gadolinium reduces short-term stretch-induced muscle damage in isolated mdx mouse muscle fibres. *J Physiol* **552**, 449–458.

Yeung EW, Whitehead NP, Suchyna TM, Gottlieb PA, Sachs F & Allen DG (2005). Effects of stretch-activated channel blockers on $[Ca^{2+}]_i$ and muscle damage in the mdx mouse. *J Physiol* **562**, 367–380.

Acknowledgements